

^{164}Pb : A possible heaviest $N = Z$ doubly-magic nucleusTomoya Naito (内藤智也),^{1,2,*} Masaaki Kimura (木村真明),^{3,†} and Masaki Sasano (笹野匡紀)^{3,‡}¹RIKEN Interdisciplinary Theoretical and Mathematical Sciences Program (iTHEMS), Wako 351-0198, Japan²Department of Physics, Graduate School of Science,
The University of Tokyo, Tokyo 113-0033, Japan³RIKEN Nishina Center for Accelerator-Based Science, Wako 351-0198, Japan

(Dated: May 21, 2024)

We confirm by using the Skyrme Hartree-Fock-Bogoliubov calculation that ^{164}Pb is a possible heaviest $N = Z$ doubly-magic nucleus whose life time is long enough to be measured on accelerator experiment. We estimate the proton-emission and alpha-decay half lives of ^{164}Pb . The estimated proton-emission half life ranges from 0.1 ps to 10 ns, while the alpha decay can be safely neglected.

Introduction.—With the advent of accelerator facilities worldwide, the nuclear chart has been rapidly extended towards the regions where the number of neutrons or protons is extremely large compared to nuclei existing in natural abundance [1, 2]. A fundamental question motivating such experimental challenges is “how far from the beta stability line nuclei can exist?”, which is related to not only the limit of our knowledge on nuclei but also exotic nuclear properties [3–6] and nucleosynthesis [7, 8].

When protons (neutrons) are added to a nucleus with keeping its neutron (proton) number, the dripline is defined by the point where the proton (neutron) separation energy becomes zero or negative. The nuclei outside the neutron dripline cannot be bound and their half lives are too short to be measured. In contrast, the nuclei outside the proton dripline may have long half lives enough to be detected because the proton mean field has the so-called Coulomb barrier, which keeps protons inside the barrier for a long time. It has been studied that there are characteristic properties, such as neutron halo [9–12] and di-neutron correlation [13–16], in neutron-rich nuclei. Then, it is an interesting question whether characteristic properties exist in proton-rich nuclei. For instance, the diproton decay [17–19] has been studied theoretically. It should also be noted that proton-rich nuclei can exist even above the threshold, in contrast to the neutron-rich nuclei.

In this regard, it is important to explore proton-rich nuclei outside the proton dripline whose life is long enough to be investigated by accelerator experiments. Doubly-magic nuclei should be primary candidates due to their stability. Up to now, ^{100}Sn is known as the heaviest $N = Z$ doubly-magic nucleus. The candidate of the next $N = Z$ doubly-magic nucleus is ^{164}Pb ($Z = N = 82$), while it is expected to be outside of the proton dripline [20, 21]; hence, it has not been carefully studied in the literature.

Nuclear shell structure is the most important quantum effect to stabilize the nuclei. Its behaviours in unstable nuclei, in particular, the appearance/disappearance of magic numbers has been studied, mainly, in the neutron-rich side [22, 23]. For example, it is recently shown that $N = 20$ magicity does not hold any more for ^{28}O [24]. Then, a question arises: “How about the magic numbers in proton-rich side?”

In this Letter, to seek the possibility of the long life of ^{164}Pb and whether $Z = N = 82$ magicity holds, we investigate this nucleus using the Skyrme Hartree-Fock-Bogoliubov (HFB) calculation [25] with continuum. Then, the half life of the one-proton emission is estimated by using the Wentzel-Kramers-Brillouin (WKB) approximation [26–28]. The alpha-decay half life is also estimated by using a phenomenological formula [29].

Calculation Method.—We perform the Skyrme HFB calculations [25, 30] with typical six Skyrme energy density functionals (EDF)—SLy4 [31], SLy5 [31], SkM* [32], UNEDF0 [33], UNEDF1 [34], and UNEDF2 [35]. The volume-type pairing interaction is used, where the cut-off energy is 60 MeV in the Hartree-Fock equivalent energy [36] and the pairing strength is determined to reproduce the neutron pairing gap of ^{120}Sn as 1.4 MeV [37]. The spherical symmetry is assumed in the calculation [38]. The radial coordinate is discretized and the HFB eigenvalue is obtained by diagonalizing the single-particle HFB Hamiltonian. Consequently, the pairing correlation with continuum is considered automatically.

We calculated with 160×0.1 fm and 240×0.1 fm box sizes, and found that the 160×0.1 fm box yields converged results. We also performed the Hartree-Fock calculation with 480×0.1 fm box to evaluate the proton-decay half-life of ^{164}Pb with the WKB approximation.

Binding energy and magicity.—In order to calculate the two-proton separation energy S_{2p} and the α -decay Q -value Q_α , we also calculate ^{160}Hg and ^{162}Hg , as well as ^{164}Pb . Once the energies of these nuclei E are obtained, S_{2p} and Q_α of ^{164}Pb are, respectively, calculated by

$$S_{2p} = E(^{162}\text{Hg}) - E(^{164}\text{Pb}), \quad (1a)$$

$$Q_\alpha = E(^{164}\text{Pb}) - E(^{160}\text{Hg}) - E(^4\text{He}). \quad (1b)$$

* tnaito@ribf.riken.jp

† masaaki.kimura@ribf.riken.jp

‡ sasano@ribf.riken.jp

The experimental value 28.2957 MeV [39, 40] is used for $E(^4\text{He})$.

The one-proton separation energy S_p is defined by

$$S_p = E(^{163}\text{Tl}) - E(^{164}\text{Pb}). \quad (2)$$

In this work, the energy of ^{163}Tl is estimated in an approximated way; the three-point formula for the pairing gap for ^{163}Tl is given by [41]

$$\Delta_p(^{163}\text{Tl}) \simeq -\frac{E(^{162}\text{Hg}) - 2E(^{163}\text{Tl}) + E(^{164}\text{Pb})}{2}. \quad (3)$$

Consequently, $E(^{163}\text{Tl})$ reads

$$E(^{163}\text{Tl}) \simeq \frac{E(^{162}\text{Hg}) + E(^{164}\text{Pb})}{2} + \Delta_p(^{163}\text{Tl}). \quad (4)$$

According to Ref. [41], Δ_p is a smooth function except at the magic numbers; hence, we take an additional approximation $\Delta_p(^{163}\text{Tl}) \simeq \Delta_p(^{162}\text{Hg})$, and accordingly, $E(^{163}\text{Tl})$ is approximated as

$$E(^{163}\text{Tl}) \simeq \frac{E(^{162}\text{Hg}) + E(^{164}\text{Pb})}{2} + \Delta_p(^{162}\text{Hg}). \quad (5)$$

The pairing gap Δ_p is estimated by the average gap [41]

$$\Delta_p = \frac{\int \tilde{V}_p(\mathbf{r}) \rho_p(\mathbf{r}) d\mathbf{r}}{\int \rho_p(\mathbf{r}) d\mathbf{r}} = \frac{\int \tilde{V}_p(\mathbf{r}) \rho_p(\mathbf{r}) d\mathbf{r}}{Z}, \quad (6)$$

where \tilde{V}_p is the pairing mean field for protons and ρ_p is the proton density [42].

In order to examine which EDFs are most appropriate, the same prescription is applied to ^{100}Sn , whose results are shown in the supplemental material [43]. The difference between theories and experiment in S_{2p} and Q_α are at most 1 and 3.5 MeV, respectively. The accuracy of S_p also depends on the approximation given in Eq. (S.1), which is the generalized version of Eq. (5). The theoretical values of S_p are within 1 MeV difference from the experimental data, which validates the approximation given in Eqs. (5) and (S.1). Thus, these six EDFs give reasonable results, while SLy4, SLy5, and UNEDF0 are more accurate. Therefore, hereinafter, we mainly refer the results obtained by the SLy4.

Table I shows the results for ^{164}Pb and Fig. 1 show the proton single-particle spectra. The proton lowest unoccupied orbital is the $2f_{7/2}$, whose energy is approximately 8 MeV, and the pairing gap of ^{164}Pb is less than 10 keV. Hence, the $Z = 82$ shell gap is large enough. Furthermore, in the supplemental material [43], the $N = Z$ nuclei are calculated within the axial deformation [36]. The systematics of Δ , S_{2p} , Q_α , and the deformation parameter β_2 also show that ^{164}Pb is a typical doubly-magic nucleus. Therefore, we conclude that $Z = N = 82$ magicity still holds.

Despite considerable neutron deficiency, the single-particle spectra are still similar to those of stable isotopes as shown in Fig. 1. The proton highest occupied single-particle orbital is the $3s_{1/2}$ and the proton single-particle orbitals of the *sdg*-shell shown in Fig. 2 behave similarly to the bound orbitals and localized in $r \lesssim 10$ fm, inside the Coulomb barrier. The bottom of the proton mean field is about 20 MeV higher than the neutron one (see Fig. 3). Accordingly, the neutron single-particle energies are also about 20 MeV deeper. This leads to the large asymmetry in the proton-neutron distribution at the central region (see Fig. 4).

The density distribution of ^{164}Pb is shown in Fig. 4. The proton and neutron root-mean-square radii, R_p and R_n , and the charge radii R_{ch} calculated by using Eq. (2) of Ref. [37] are summarized in Table I. Because of the strong Coulomb repulsion, R_p is much larger than R_n and the proton skin $R_p - R_n$ reaches 0.1 fm. The peak position of $4\pi r^2 \rho_p$ is also about 0.1 fm outside of $4\pi r^2 \rho_n$, which is consistent with the proton-skin thickness.

As all the EDFs yield $S_p < 0$, $S_{2p} < 0$, and $Q_\alpha > 0$, one- and two-proton emission, and the α decay channels should be open as summarized in Fig. 5. Since the proton highest single-particle orbital is the $3s_{1/2}$, the $1p$ emission from this orbital should dominate and $2p$ -emission process is negligible.

One-proton emission half life.—The one-proton emission half life is estimated by the WKB approximation. As discussed above, we assume that a $3s_{1/2}$ proton is emitted.

The WKB approximation for one-proton emission half life is given by [26–28]

$$T_{1/2}^p = \frac{\hbar c \log 2}{S\Gamma} \text{ fm}/c, \quad (7)$$

where the spectroscopic factor $S = 2$ is for the $3s_{1/2}$ protons and the decay width Γ is calculated by

$$\Gamma = N \frac{(\hbar c)^2}{4\mu c^2} \exp \left[-2 \int_{r_1}^{r_2} k(r) dr \right] \text{ MeV}. \quad (8)$$

Here, μ is the nucleon reduced mass, N is the normalization factor given by

$$N^{-1} = \int_0^{r_1} \frac{1}{k(r)} \cos^2 \left[\int_0^r k(r') dr' - \frac{\pi}{4} \right] dr \text{ fm}^2, \quad (9)$$

and

$$k(r) = \frac{\sqrt{2\mu c^2 |E - V(r)|}}{\hbar c} \text{ fm}^{-1}. \quad (10)$$

In this calculation, $\varepsilon_{\pi 3s_{1/2}}$ is used for E and the proton mean-field potential shown in Fig. 3 is used for $V(r)$. We use the bare proton mass m_p for μ for simplicity. Note that another choice for E is $-S_p$, but it is smaller than $\varepsilon_{\pi 3s_{1/2}}$; hence, this choice always gives longer life

TABLE I. Calculation results for ^{164}Pb . These calculation results are obtained by the Skyrme Hartree-Fock-Bogoloubov calculation with SLy4 [31], SLy5 [31], SkM* [32], UNEDF0 [33], UNEDF1 [34], and UNEDF2 [35] EDFs and the volume-type pairing interaction. All the results except R_p , R_n , or R_{ch} are shown in MeV, while R_p , R_n , or R_{ch} are shown in fm.

EDF	SLy4	SLy5	SkM*	UNEDF0	UNEDF1	UNEDF2
$E(^{164}\text{Pb})$	-1208.3863	-1207.4446	-1198.3397	-1207.5137	-1210.0435	-1210.2978
$E(^{162}\text{Hg})$	-1213.3723	-1212.4313	-1203.2334	-1213.0773	-1215.8523	-1215.7930
$E(^{160}\text{Hg})$	-1180.8988	-1180.0439	-1170.4134	-1181.5332	-1184.0256	-1183.3580
$E(^{163}\text{Tl})$	-1210.1707	-1209.2717	-1200.2815	-1209.7663	-1212.3952	-1212.4658
S_p	-1.7843	-1.8271	-1.9419	-2.2525	-2.3517	-2.1680
S_{2p}	-4.9860	-4.9867	-4.8937	-5.5636	-5.8088	-5.4952
Q_α	0.8081	0.8950	0.3694	2.3151	2.2778	1.3558
$\Delta_p(^{164}\text{Pb})$	0.0004	0.0004	0.0002	0.0003	0.0004	0.0004
$\Delta_n(^{164}\text{Pb})$	0.0005	0.0004	0.0001	0.0012	0.0008	0.0006
$\Delta_p(^{162}\text{Hg})$	0.7086	0.6662	0.5050	0.5293	0.5528	0.5796
$\Delta_n(^{162}\text{Hg})$	0.0017	0.0012	0.0008	0.0031	0.0028	0.0018
$\varepsilon_{\pi 1g_{7/2}}$	-2.0381	-2.1416	-0.8348	+0.6652	-0.3438	-0.3199
$\varepsilon_{\pi 2d_{5/2}}$	-0.6997	-0.7006	-0.1450	+0.5489	+0.7821	+0.7275
$\varepsilon_{\pi 2d_{3/2}}$	+1.4265	+1.4259	+2.0222	+2.3336	+2.3513	+2.2581
$\varepsilon_{\pi 1h_{11/2}}$	+1.6565	+1.7577	+1.6221	+2.1503	+2.3665	+1.8482
$\varepsilon_{\pi 3s_{1/2}}$	+1.9030	+1.8969	+2.3310	+2.5316	+2.8762	+2.9433
R_p	5.2099	5.2028	5.2091	5.2036	5.1928	5.1928
R_n	5.0911	5.0834	5.0834	5.0937	5.0937	5.0922
R_{ch}	5.2673	5.2603	5.2665	5.2611	5.2504	5.2503

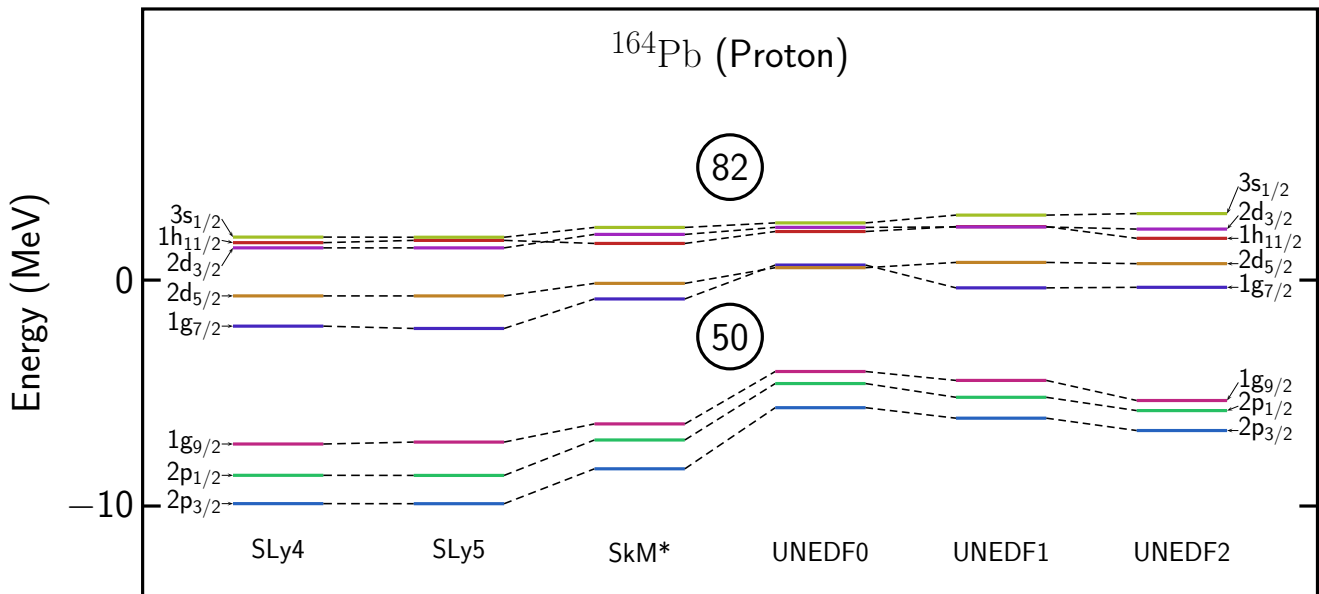


FIG. 1. Proton single-particle spectra of ^{164}Pb calculated by using the Skyrme Hartree-Fock-Bogoliubov calculation with 160×0.1 fm box. The single-particle energies plotted here are the eigenvalues of the p - h Hamiltonian.

time. Here, r_1 and r_2 ($r_1 < r_2$) are the classical turning point [44] of a particle with the energy $E = \varepsilon_{\pi 3s_{1/2}}$ in the mean-field $V(r)$, i.e., the crossing point of the solid and dotted lines in Fig. 3. In SLy4, SLy5, and SkM*, r_2 is outside of the cutoff radius. Therefore, we estimate $r_2 = 81e^2/\varepsilon_{\pi 3s_{1/2}}$ [45].

The estimations of the life time are summarized in Table II. As can be seen, r_1 is almost always 7.5 fm, while r_2

depends on the EDFs because they give different $\varepsilon_{\pi 3s_{1/2}}$. Accordingly, the estimated half lives range from the order of 0.1 ps to 10 ns. Especially, if $\varepsilon_{\pi 3s_{1/2}}$ is small enough, as in the SLy4, SLy5, and SkM* cases, it is possible to measure properties of ^{164}Pb before its decay by accelerator experiments.

Model analysis for the WKB approximation.—To elucidate the relation between the $1p$ -proton emission half life

TABLE II. Proton-emission and alpha-decay half lives, $T_{1/2}^p$ and $T_{1/2}^\alpha$, for ^{164}Pb , where $T_{1/2}^p$ and $T_{1/2}^\alpha$ are estimated by using the WKB approximation and the phenomenological formula [29], respectively. The third crossing point r_2 is given by the numerical calculation for the UNEDF series, while it is estimated by the proton-daughter nucleus Coulomb potential for the others. See the main text for the detail.

EDF	SLy4	SLy5	SkM*	UNEDF0	UNEDF1	UNEDF2
r_1 (fm)	7.5	7.5	7.5	7.5	7.5	7.4
r_2 (fm)	61.3	61.5	50.0	46.6	41.1	40.0
$\varepsilon_{\pi 3s_{1/2}}$ (MeV)	+1.9	+1.9	+2.3	+2.5	+2.9	+2.9
N^{-1} (fm ²)	3.5	3.5	3.0	4.1	3.5	3.1
Γ ($\times 10^{-13}$ MeV)	0.20	0.18	56	290	7000	13000
$T_{1/2}^p$ (ps)	11000	13000	41	7.8	0.33	0.18
Q_α (MeV)	0.81	0.90	0.37	2.3	2.3	1.4
$\log_{10} T_{1/2}^\alpha$ (\log_{10} s)	98	90	170	36	37	63

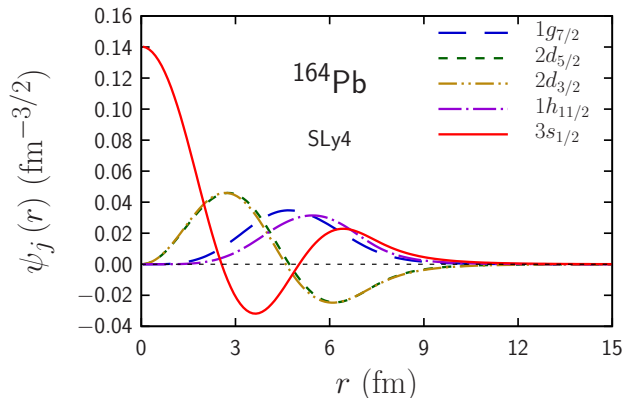


FIG. 2. Proton single-particle orbitals of ^{164}Pb calculated by using the Skyrme Hartree-Fock calculation with 480×0.1 fm box with the SLy4 EDF.

and the single-particle energy of the proton $3s_{1/2}$ orbital,

we approximate the proton mean field by a simplified potential given by

$$V(r) = \begin{cases} -40 \text{ MeV} & \text{for } r < 7.5 \text{ fm,} \\ 81e^2/r & \text{otherwise,} \end{cases} \quad (11)$$

where the classical turning points are set as $r_1 = 7.5$ fm and $r_2 = 81e^2/\varepsilon_{\pi 3s_{1/2}}$. By the WKB approximation with this potential, we estimated the half life as a function of $\varepsilon_{\pi 3s_{1/2}}$ as shown in Fig. 6. It reasonably explains the estimation from more realistic HFB potential indicating that the half life is not sensitive to the detail of the potential. Thus, as expected, the half life is roughly determined by only the single-particle energy of the proton $3s_{1/2}$ orbital. In turn, this means that the measurement of the half life will provide an estimation of the proton single-particle energy $\varepsilon_{\pi 3s_{1/2}}$.

Alpha-decay half life.—Lastly, we estimate the α -decay half life $T_{1/2}^\alpha$. We use a phenomenological formula proposed in Ref. [29]

$$\log_{10} T_{1/2}^\alpha = \frac{2 \log_{10} e}{\hbar c} \sqrt{2M_\alpha \frac{A-4}{A}} \int_R^b \sqrt{V_C(r) - Q_\alpha} dr - \log_{10} N - \log_{10} (\log_2 e) \log_{10} s \quad (12)$$

with

$$V_C(r) = \frac{2Z_D e^2}{r}, \quad (13a)$$

$$b = \frac{2Z_D e^2}{Q_\alpha} \quad (13b)$$

where $A = 164$ is the mass number of the parent nucleus, $Z_D = 80$ is the proton number of the daughter nucleus, and M_α is the mass of the α particle. The parameter $-\log_{10} N = -21.4577$ is related to the penetration factor and the preformation probability; R is the position where the penetration of the potential barrier begins and $R = r_0 A_D^{1/3} + d_0$, $r_0 = 1.08$ fm, $d_0 = 2.0$ fm are used in this

calculation with the mass number of the daughter nucleus $A_D = 160$. The estimated values of $T_{1/2}^\alpha$ are shown in Table II. It can be seen that $T_{1/2}^\alpha$ is more than 10^{35} s; thus, we need not to consider the α decay of ^{164}Pb . Note that even if the deformation is considered, Q_α does not change much and hence, the conclusion does not change.

Summary.—Using the Skyrme Hartree-Fock-Bogoliubov calculation, we confirmed that ^{164}Pb nucleus is a possible heaviest $N = Z$ doubly-magic nucleus. The proton-emission half life is estimated by using the Wentzel-Kramers-Brillouin approximation. The estimated half life ranges from 0.1 ps to 10 ns, which depends on the single-particle energy of the proton $3s_{1/2}$

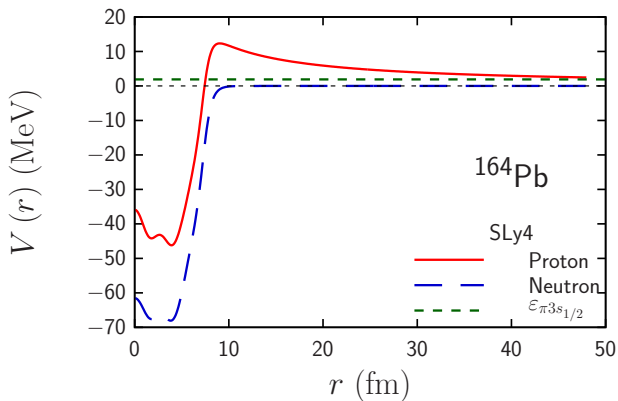


FIG. 3. Proton and neutron mean-field potentials of ^{164}Pb calculated by using the Skyrme Hartree-Fock calculation with 480×0.1 fm box with the SLy4 EDF. The single-particle energy of the proton $3s_{1/2}$ orbital, $\varepsilon_{\pi 3s_{1/2}}$, is shown in the green dotted line.

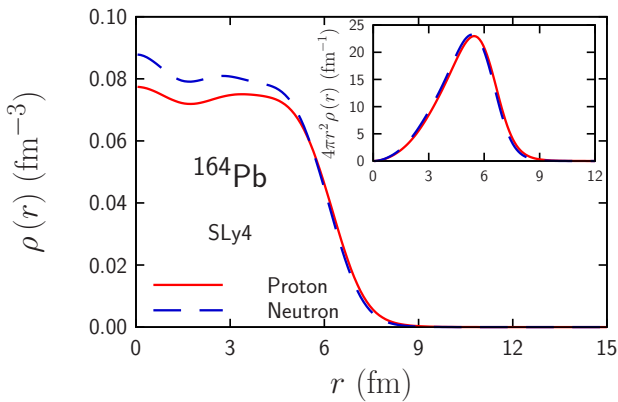


FIG. 4. Proton and neutron densities of ^{164}Pb calculated by using the Skyrme Hartree-Fock calculation with 480×0.1 fm box with the SLy4 EDF.

orbital. There is a one-to-one correspondence between the proton single-particle energy of the $3s_{1/2}$ orbital and the proton-emission half life. If the single-particle energy is lower, the half life is longer and it may be possible to investigate properties of ^{164}Pb experimentally. In turn, once the proton-emission half life is measured, the proton single-particle energy can be estimated, which will impose a constraint on the energy density functionals. The alpha-decay half life is estimated to be longer than 10^{35} s, which is much longer than the age of the Universe; hence, the alpha decay of ^{164}Pb can be safely neglected although the alpha-decay channel is opened. The recent experiment [46] predicted that the $N = 82$ magic number is still robust in the neutron deficient side. Our finding also supports this prediction, and the synthesis of ^{164}Pb at next-generation accelerator facilities is demanded.

The authors acknowledge for the fruitful discussion

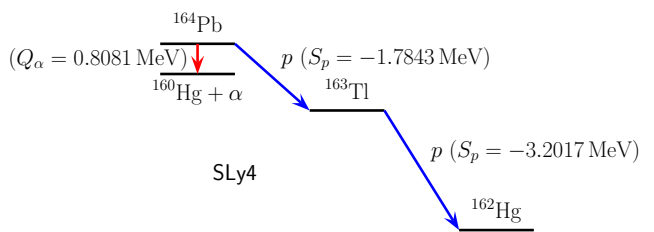


FIG. 5. Decay scheme of ^{164}Pb calculated by using the Skyrme Hartree-Fock calculation with 160×0.1 fm box with the SLy4 EDF.

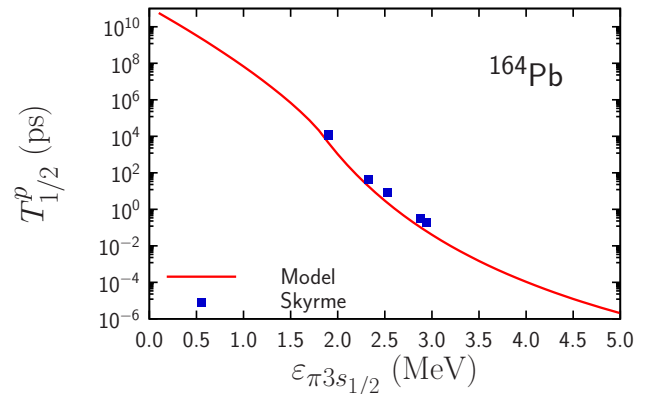


FIG. 6. One-proton emission half life $T_{1/2}^p$ calculated with the model potential (solid line) and the WKB method (squares). See the text for the detail.

with Shintaro Go, Hiroyuki Koura, Hiroyuki Sagawa, Hiroyoshi Sakurai, Daisuke Suzuki, and the members of the RIBF Future Plan Working Group. T. N. acknowledges the RIKEN Special Postdoctoral Researcher Program, the JSPS Grant-in-Aid for Research Activity Start-up under Grant No. JP22K20372, the JSPS Grant-in-Aid for Transformative Research Areas (A) under Grant No. JP23H04526, the JSPS Grant-in-Aid for Scientific Research (B) under Grant Nos. JP23H01845 and JP23K01845, the JSPS Grant-in-Aid for Scientific Research (C) under Grant No. JP23K03426, and the JSPS Grant-in-Aid for Early-Career Scientists under Grant No. JP24K17057. The numerical calculations were performed on cluster computers at the RIKEN iTHEMS program.

-
- [1] T. Nakamura, H. Sakurai, and H. Watanabe, Exotic nuclei explored at in-flight separators, *Prog. Part. Nucl. Phys.* **97**, 53 (2017).
 - [2] H. Sakurai, Nuclear physics with RI Beam Factory, *Front. Phys.* **13**, 132111 (2018).
 - [3] R. F. Casten and B. M. Sherrill, The Study of Exotic Nuclei, *Prog. Part. Nucl. Phys.* **45**, S171 (2000).

- [4] N. Paar, The quest for novel modes of excitation in exotic nuclei, *J. Phys. G* **37**, 064014 (2010).
- [5] S.-G. Zhou, Structure of Exotic Nuclei: a Theoretical Review, *Proc. Sci.* **281**, 373 (2017).
- [6] H. Nakada, Properties of exotic nuclei and their linkage to the nucleonic interaction, *Int. J. Mod. Phys. E* **29**, 1930008 (2020).
- [7] K. Nomoto, C. Kobayashi, and N. Tominaga, Nucleosynthesis in Stars and the Chemical Enrichment of Galaxies, *Annu. Rev. Astron. Astrophys.* **51**, 457 (2013).
- [8] M. R. Mumpower, R. Surman, G. C. McLaughlin, and A. Aprahamian, The impact of individual nuclear properties on r-process nucleosynthesis, *Prog. Part. Nucl. Phys.* **86**, 86 (2016).
- [9] I. Tanihata, H. Hamagaki, O. Hashimoto, Y. Shida, N. Yoshikawa, K. Sugimoto, O. Yamakawa, T. Kobayashi, and N. Takahashi, Measurements of Interaction Cross Sections and Nuclear Radii in the Light p -Shell Region, *Phys. Rev. Lett.* **55**, 2676 (1985).
- [10] I. Tanihata, H. Savajols, and R. Kanungo, Recent experimental progress in nuclear halo structure studies, *Prog. Part. Nucl. Phys.* **68**, 215 (2013).
- [11] N. Kobayashi, T. Nakamura, Y. Kondo, J. A. Tostevin, Y. Utsuno, N. Aoi, H. Baba, R. Barthelemy, M. A. Famiano, N. Fukuda, N. Inabe, M. Ishihara, R. Kanungo, S. Kim, T. Kubo, G. S. Lee, H. S. Lee, M. Matsushita, T. Motobayashi, T. Ohnishi, N. A. Orr, H. Otsu, T. Otsuka, T. Sako, H. Sakurai, Y. Satou, T. Sumikama, H. Takeda, S. Takeuchi, R. Tanaka, Y. Togano, and K. Yoneda, Observation of a p -Wave One-Neutron Halo Configuration in ^{37}Mg , *Phys. Rev. Lett.* **112**, 242501 (2014).
- [12] S. Bagchi, R. Kanungo, Y. K. Tanaka, H. Geissel, P. Doornenbal, W. Horiuchi, G. Hagen, T. Suzuki, N. Tsunoda, D. S. Ahn, H. Baba, K. Behr, F. Browne, S. Chen, M. L. Cortés, A. Estradé, N. Fukuda, M. Holl, K. Itahashi, N. Iwasa, G. R. Jansen, W. G. Jiang, S. Kaur, A. O. Macchiavelli, S. Y. Matsumoto, S. Momiyama, I. Murray, T. Nakamura, S. J. Novario, H. J. Ong, T. Otsuka, T. Papenbrock, S. Paschalis, A. Prochazka, C. Scheidenberger, P. Schrock, Y. Shimizu, D. Steppenbeck, H. Sakurai, D. Suzuki, H. Suzuki, M. Takechi, H. Takeda, S. Takeuchi, R. Taniuchi, K. Wimmer, and K. Yoshida, Two-Neutron Halo is Unveiled in ^{29}F , *Phys. Rev. Lett.* **124**, 222504 (2020).
- [13] K. Hagino and H. Sagawa, Three-body model calculation of the 2^+ state in ^{26}O , *Phys. Rev. C* **90**, 027303 (2014).
- [14] Y. Kubota, A. Corsi, G. Authalet, H. Baba, C. Caesar, D. Calvet, A. Delbart, M. Dozono, J. Feng, F. Flaviigny, J.-M. Gheller, J. Gibelin, A. Giganon, A. Gillibert, K. Hasegawa, T. Isobe, Y. Kanaya, S. Kawakami, D. Kim, Y. Kikuchi, Y. Kiyokawa, M. Kobayashi, N. Kobayashi, T. Kobayashi, Y. Kondo, Z. Korkulu, S. Koyama, V. Lapoux, Y. Maeda, F. M. Marqués, T. Motobayashi, T. Miyazaki, T. Nakamura, N. Nakatsuka, Y. Nishio, A. Obertelli, K. Ogata, A. Ohkura, N. A. Orr, S. Ota, H. Otsu, T. Ozaki, V. Panin, S. Paschalis, E. C. Pollacco, S. Reichert, J.-Y. Rousse, A. T. Saito, S. Sakaguchi, M. Sako, C. Santamaria, M. Sasano, H. Sato, M. Shikata, Y. Shimizu, Y. Shindo, L. Stuhl, T. Sumikama, Y. L. Sun, M. Tabata, Y. Togano, J. Tsubota, Z. H. Yang, J. Yasuda, K. Yoneda, J. Zenihiro, and T. Uesaka, Surface Localization of the Dineutron in ^{11}Li , *Phys. Rev. Lett.* **125**, 252501 (2020).
- [15] T. Furumoto, T. Suhara, and N. Itagaki, Drastic change of inelastic scattering dependent on the development of dineutron correlations in ^{10}Be , *Phys. Rev. C* **104**, 034613 (2021).
- [16] M. Yamagami, Momentum-space structure of dineutrons in Borromean nuclei, *Phys. Rev. C* **106**, 044316 (2022).
- [17] L. V. Grigorenko, R. C. Johnson, I. G. Mukha, I. J. Thompson, and M. V. Zhukov, Two-proton radioactivity and three-body decay: General problems and theoretical approach, *Phys. Rev. C* **64**, 054002 (2001).
- [18] E. Olsen, M. Pfützner, N. Birge, M. Brown, W. Nazarewicz, and A. Perhac, Landscape of Two-Proton Radioactivity, *Phys. Rev. Lett.* **110**, 222501 (2013).
- [19] E. Olsen, M. Pfützner, N. Birge, M. Brown, W. Nazarewicz, and A. Perhac, Erratum: Landscape of Two-Proton Radioactivity [*Phys. Rev. Lett.* **110**, 222501 (2013)], *Phys. Rev. Lett.* **111**, 139903 (2013).
- [20] H. Koura, T. Tachibana, M. Uno, and M. Yamada, Nucleidic Mass Formula on a Spherical Basis with an Improved Even-Odd Term, *Prog. Theor. Phys.* **113**, 305 (2005).
- [21] P. Möller, A. J. Sierk, T. Ichikawa, and H. Sagawa, Nuclear ground-state masses and deformations: FRDM (2012), *At. Data Nucl. Data Tables* **109**, 1 (2016).
- [22] O. Sorlin and M.-G. Porquet, Nuclear magic numbers: New features far from stability, *Prog. Part. Nucl. Phys.* **61**, 602 (2008).
- [23] J. J. Li, J. Margueron, W. H. Long, and N. Van Giai, Magicity of neutron-rich nuclei within relativistic self-consistent approaches, *Phys. Lett. B* **753**, 97 (2016).
- [24] Y. Kondo, N. L. Achouri, H. A. Falou, L. Atar, T. Aumann, H. Baba, K. Boretzky, C. Caesar, D. Calvet, H. Chae, N. Chiga, A. Corsi, F. Delaunay, A. Delbart, Q. Deshayes, Z. Dombrádi, C. A. Douma, A. Ekström, Z. Elekes, C. Forssén, I. Gašparić, J. M. Gheller, J. Gibelin, A. Gillibert, G. Hagen, M. N. Harakeh, A. Hirayama, C. R. Hoffman, M. Holl, A. Horvat, A. Horváth, J. W. Hwang, T. Isobe, W. G. Jiang, J. Kahlbow, N. Kalantar-Nayestanaki, S. Kawase, S. Kim, K. Kisamori, T. Kobayashi, D. Körper, S. Koyama, I. Kuti, V. Lapoux, S. Lindberg, F. M. Marqués, S. Masuoka, J. Mayer, K. Miki, T. Murakami, M. Najafi, T. Nakamura, K. Nakano, N. Nakatsuka, T. Nilsson, A. Obertelli, K. Ogata, F. de Oliveira Santos, N. A. Orr, H. Otsu, T. Otsuka, T. Ozaki, V. Panin, T. Papenbrock, S. Paschalis, A. Revel, D. Rossi, A. T. Saito, T. Y. Saito, M. Sasano, H. Sato, Y. Satou, H. Scheit, F. Schindler, P. Schrock, M. Shikata, N. Shimizu, Y. Shimizu, H. Simon, D. Sohler, O. Sorlin, L. Stuhl, Z. H. Sun, S. Takeuchi, M. Tanaka, M. Thoennessen, H. Törnqvist, Y. Togano, T. Tomai, J. Tscheuschner, J. Tsubota, N. Tsunoda, T. Uesaka, Y. Utsuno, I. Vernon, H. Wang, Z. Yang, M. Yasuda, K. Yoneda, and S. Yoshida, First observation of ^{28}O , *Nature* **620**, 965 (2023).
- [25] D. Vautherin and D. M. Brink, Hartree-Fock Calculations with Skyrme's Interaction. I. Spherical Nuclei, *Phys. Rev. C* **5**, 626 (1972).
- [26] B. Buck, A. C. Merchant, and S. M. Perez, Ground state proton emission from heavy nuclei, *Phys. Rev. C* **45**, 1688 (1992).
- [27] S. Åberg, P. B. Semmes, and W. Nazarewicz, Spherical proton emitters, *Phys. Rev. C* **56**, 1762 (1997).
- [28] Y. Xiao, S.-Z. Xu, R.-Y. Zheng, X.-X. Sun, L.-S. Geng,

- and S.-S. Zhang, One-proton emission from $^{148-151}\text{Lu}$ in the DRHBc+WKB approach, *Phys. Lett. B* **845**, 138160 (2023).
- [29] H. Koura, Phenomenological formula for alpha-decay half-lives, *J. Nucl. Sci. Technol.* **49**, 816 (2012).
- [30] J. Dobaczewski, H. Flocard, and J. Treiner, Hartree-Fock-Bogolyubov description of nuclei near the neutron-drip line, *Nucl. Phys. A* **422**, 103 (1984).
- [31] E. Chabanat, P. Bonche, P. Haensel, J. Meyer, and R. Schaeffer, A Skyrme parametrization from subnuclear to neutron star densities Part II. Nuclei far from stabilities, *Nucl. Phys. A* **635**, 231 (1998).
- [32] J. Bartel, P. Quentin, M. Brack, C. Guet, and H.-B. Håkansson, Towards a better parametrisation of Skyrme-like effective forces: A critical study of the SkM force, *Nucl. Phys. A* **386**, 79 (1982).
- [33] M. Kortelainen, T. Lesinski, J. Moré, W. Nazarewicz, J. Sarich, N. Schunck, M. V. Stoitsov, and S. Wild, Nuclear energy density optimization, *Phys. Rev. C* **82**, 024313 (2010).
- [34] M. Kortelainen, J. McDonnell, W. Nazarewicz, P.-G. Reinhard, J. Sarich, N. Schunck, M. V. Stoitsov, and S. M. Wild, Nuclear energy density optimization: Large deformations, *Phys. Rev. C* **85**, 024304 (2012).
- [35] M. Kortelainen, J. McDonnell, W. Nazarewicz, E. Olsen, P.-G. Reinhard, J. Sarich, N. Schunck, S. M. Wild, D. Davesne, J. Erler, and A. Pastore, Nuclear energy density optimization: Shell structure, *Phys. Rev. C* **89**, 054314 (2014).
- [36] R. Navarro Perez, N. Schunck, R.-D. Lasserri, C. Zhang, and J. Sarich, Axially deformed solution of the Skyrme–Hartree–Fock–Bogolyubov equations using the transformed harmonic oscillator basis (III) HFBTHO (v3.00): A new version of the program, *Comput. Phys. Commun.* **220**, 363 (2017).
- [37] T. Naito, T. Oishi, H. Sagawa, and Z. Wang, Comparative study on charge radii and their kinks at magic numbers, *Phys. Rev. C* **107**, 054307 (2023).
- [38] In the Supplemental Material [43], the Skyrme HFB calculation with considering the axial deformation using the harmonic-oscillator basis is performed using the HFBTHO code [36]. Actually, it was confirmed that ^{164}Pb is spherical and shows doubly-magic properties even if the axial deformation is considered.
- [39] W. J. Huang, M. Wang, F. G. Kondev, G. Audi, and S. Naimi, The AME 2020 atomic mass evaluation (I). Evaluation of input data, and adjustment procedures, *Chin. Phys. C* **45**, 030002 (2021).
- [40] M. Wang, W. J. Huang, F. G. Kondev, G. Audi, and S. Naimi, The AME 2020 atomic mass evaluation (II). Tables, graphs and references, *Chin. Phys. C* **45**, 030003 (2021).
- [41] M. Bender, K. Rutz, P.-G. Reinhard, and J. A. Maruhn, Pairing gaps from nuclear mean-field models, *Eur. Phys. J. A* **8**, 59 (2000).
- [42] Another way to calculate the pairing gap Δ_p (^{162}Hg) is the spectral gap
- $$\tilde{\Delta}_p = \frac{\int \tilde{V}_p(\mathbf{r}) \tilde{\rho}_p(\mathbf{r}) d\mathbf{r}}{\int \tilde{\rho}_p(\mathbf{r}) d\mathbf{r}} \quad (14)$$
- where $\tilde{\rho}_p$ is the proton pair density. The results do not change much even if we use the spectral gap instead.
- [43] See Supplemental Material at [URL will be inserted by publisher] for calculation results of ^{100}Sn and calculation results of $N = Z$ nuclei given within the axial deformation.
- [44] In Refs. [26–28], another crossing point $r_0 < r_1$ also appears. This is due to the centrifugal core, while we consider the proton $3s_{1/2}$ orbital and hence this barrier does not exist.
- [45] We confirm that the proton mean-field potential can be well described with the Coulomb potential in $r \gtrsim 10$ fm.
- [46] H. B. Yang, Z. G. Gan, Y. J. Li, M. L. Liu, S. Y. Xu, C. Liu, M. M. Zhang, Z. Y. Zhang, M. H. Huang, C. X. Yuan, S. Y. Wang, L. Ma, J. G. Wang, X. C. Han, A. Röhilla, S. Q. Zuo, X. Xiao, X. B. Zhang, L. Zhu, Z. F. Yue, Y. L. Tian, Y. S. Wang, C. L. Yang, Z. Zhao, X. Y. Huang, Z. C. Li, L. C. Sun, J. Y. Wang, H. R. Yang, Z. W. Lu, W. Q. Yang, X. H. Zhou, W. X. Huang, N. Wang, S. G. Zhou, Z. Z. Ren, and H. S. Xu, Discovery of New Isotopes ^{160}Os and ^{156}W : Revealing Enhanced Stability of the $N = 82$ Shell Closure on the Neutron-Deficient Side, *Phys. Rev. Lett.* **132**, 072502 (2024).

Supplemental Material

 ^{164}Pb : A possible heaviest $N = Z$ doubly-magic nucleusTomoya Naito (内藤智也),^{1,2} Masaaki Kimura (木村真明),³ and Masaki Sasano (笹野匡紀)³¹*RIKEN Interdisciplinary Theoretical and Mathematical Sciences Program (iTHEMS), Wako 351-0198, Japan*²*Department of Physics, Graduate School of Science,
The University of Tokyo, Tokyo 113-0033, Japan*³*RIKEN Nishina Center for Accelerator-Based Science, Wako 351-0198, Japan*

(Dated: May 21, 2024)

In this supplemental material, we show calculation results of ^{100}Sn and calculation results of $N = Z$ nuclei given within the axial deformation.

CALCULATION RESULTS FOR ^{100}Sn

The calculation results for ^{100}Sn are shown in Table S.1. The calculation setup is the same as for ^{164}Pb shown in the main text. Since the experimental data of masses are available for ^{98}Cd and ^{100}Sn in the AME2020 [1, 2], the experimental S_{2p} is also shown. Although the experimental data of masses of ^{96}Cd and ^{99}In are not available, estimated values for them are available in the AME2020. Hence, the estimated values for S_p and Q_α are also shown for the reference.

CALCULATION RESULTS FOR $N = Z$ NUCLEI USING HFBTHO CODE

To show the ^{164}Pb nucleus shows typical behaviour of a doubly-magic nucleus, we calculate the $N = Z$ even-even nuclei ($8 \leq N = Z \leq 100$) with considering the axial deformation. We use the HFBTHO code [8]. Harmonic-oscillator wave functions up to $24\hbar\omega$ are used for the basis with $\hbar\omega = 1.2 \times 41A^{-1/3}$ MeV. In order to consider the deformation properly, each nucleus is calculated with the initial Woods-Saxon potential of different deformation parameter $\beta_2 = -0.5, -0.4, \dots, +0.5$, and the result with the smallest energy is used for the further analysis.

Figure S.1 shows the pairing gap Δ and the deformation parameter β_2 for protons and neutrons. We take the SLy4 with the volume-type pairing interaction as an example. As it can be seen, the $N = Z$ nuclei with the conventional magic numbers, Z or $N = 8, 20, 28, 50$, and even 82, are spherical ($\beta_2 = 0$) without the pairing gap ($\Delta = 0$). Even

TABLE S.1. Calculation results for ^{100}Sn . These calculation results are obtained by the Skyrme Hartree-Fock-Bogolubov calculation with SLy4 [3], SLy5 [3], SkM* [4], UNEDF0 [5], UNEDF1 [6], and UNEDF2 [7] EDFs and the volume-type pairing interaction. The experimental data taken from Refs. [1, 2] are also shown, where $E(^{96}\text{Cd})$ and $E(^{99}\text{In})$ are the estimated values. All the results except R_p , R_n , or R_{ch} are shown in MeV, while R_p , R_n , or R_{ch} are shown in fm.

EDF	SLy4	SLy5	SkM*	UNEDF0	UNEDF1	UNEDF2	Expt.
$E(^{100}\text{Sn})$	-828.5887	-827.8619	-826.1837	-826.8630	-828.8568	-829.7869	-825.16260
$E(^{98}\text{Cd})$	-823.8963	-823.2002	-820.9489	-822.4334	-824.6167	-824.8113	-821.07294
$E(^{96}\text{Cd})$	-794.0282	-793.5384	-790.4066	-793.3220	-795.1982	-794.4453	-792.9
$E(^{99}\text{In})$	-825.4207	-824.7584	-822.9540	-824.0293	-826.0985	-826.5907	-822.1
S_p	3.1680	3.1036	3.2297	2.8337	2.7584	3.1962	3.1
S_{2p}	4.6924	4.6617	5.2348	4.4296	4.2401	4.9756	4.08966
Q_α	-6.2648	-6.0279	-7.4814	-5.2454	-5.3630	-7.0459	-4.0
$\Delta_p(^{100}\text{Sn})$	0.0005	0.0005	0.0003	0.0005	0.0004	0.0005	—
$\Delta_n(^{100}\text{Sn})$	0.0005	0.0004	0.0001	0.0019	0.0006	0.0003	—
$\Delta_p(^{98}\text{Cd})$	0.8218	0.7727	0.6123	0.6189	0.6383	0.7084	—
$\Delta_n(^{98}\text{Cd})$	0.0014	0.0013	0.0005	0.0035	0.0016	0.0008	—
$\varepsilon_{\pi 1f_{5/2}}$	-7.9892	-8.1391	-6.6304	-4.8840	-5.9802	-5.8387	—
$\varepsilon_{\pi 2p_{3/2}}$	-7.3229	-7.3311	-6.6013	-5.7452	-5.6142	-5.7212	—
$\varepsilon_{\pi 2p_{1/2}}$	-5.6751	-5.6918	-4.9295	-4.3633	-4.3989	-4.5109	—
R_p	4.4287	4.4231	4.4210	4.4223	4.4076	4.4069	—
R_n	4.3478	4.3418	4.3365	4.3504	4.3440	4.3420	—
R_{ch}	4.4962	4.4906	4.4885	4.4899	4.4754	4.4747	—

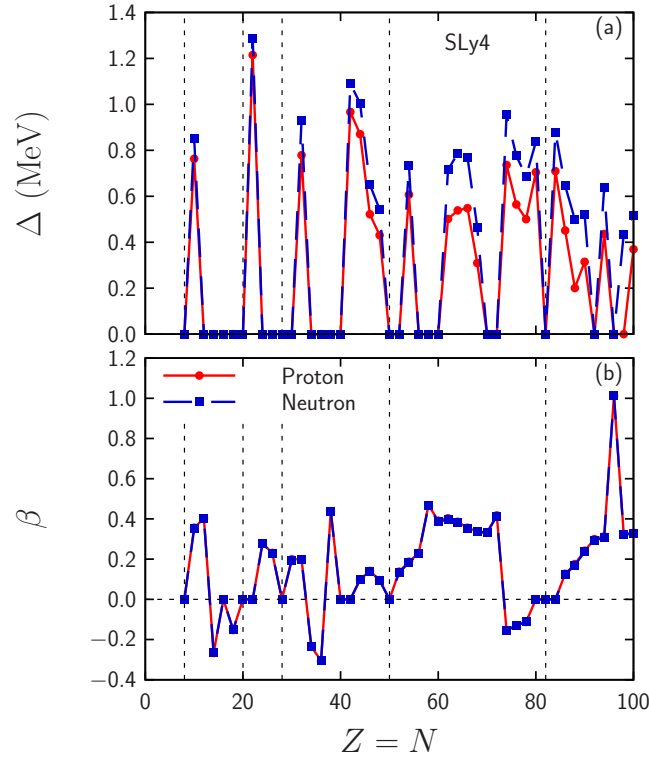


FIG. S.1. Pairing gap Δ and deformation parameter β_2 for protons (solid line) and neutrons (dashed line) calculated by using the HFBTHO code with the SLy4 EDF and the volume-type pairing interaction.

though the heavy $N = Z$ nuclei are much neutron deficient one, the deformation parameter β_2 for protons are the same as those for neutrons.

Figure S.2 shows the two-proton separation energy S_{2p} , the one-proton separation energy S_p , and the α -decay Q -value Q_α . Energies of odd- A nuclei are needed to calculate S_p ; we take the similar way to Eq. (5). However, in contrast to ^{164}Pb , there is an ambiguity which side of nucleus in Eq. (3) is magic. Therefore, we calculate the energy of an odd- A nucleus as

$$E(Z-1, N) \simeq \frac{E(Z-2, N) + E(Z, N)}{2} + \bar{\Delta}_p \quad (\text{S.1})$$

with

$$\bar{\Delta}_p = \begin{cases} \Delta_p(Z, N) & \text{if } Z-2 \text{ is magic,} \\ \Delta_p(Z-2, N) & \text{if } Z \text{ is magic,} \\ \frac{\Delta_p(Z-2, N) + \Delta_p(Z, N)}{2} & \text{otherwise,} \end{cases} \quad (\text{S.2})$$

where the magic numbers used here are conventional 8, 20, 28, 50, 82. The magic numbers, including $Z = 82$, show sudden change of S_{2p} , S_p , and Q_α . Therefore, $N = Z = 82$ behaves as the normal magic numbers.

-
- [1] W. J. Huang, M. Wang, F. G. Kondev, G. Audi, and S. Naimi, The AME 2020 atomic mass evaluation (I). Evaluation of input data, and adjustment procedures, *Chin. Phys. C* **45**, 030002 (2021).
 - [2] M. Wang, W. J. Huang, F. G. Kondev, G. Audi, and S. Naimi, The AME 2020 atomic mass evaluation (II). Tables, graphs and references, *Chin. Phys. C* **45**, 030003 (2021).
 - [3] E. Chabanat, P. Bonche, P. Haensel, J. Meyer, and R. Schaeffer, A Skyrme parametrization from subnuclear to neutron star densities Part II. Nuclei far from stabilities, *Nucl. Phys. A* **635**, 231 (1998).

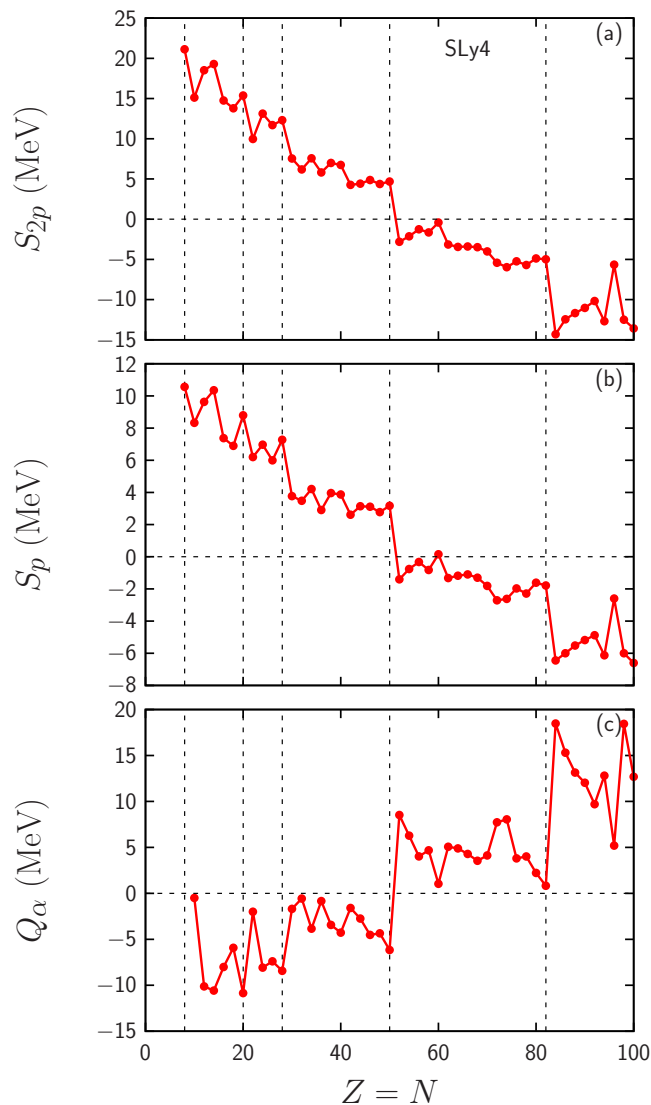


FIG. S.2. Two-proton separation energy S_{2p} , one-proton separation energy S_p , and the α -decay Q -value Q_α calculated by using the HFBTHO code with the SLy4 EDF and the volume-type pairing interaction.

- [4] J. Bartel, P. Quentin, M. Brack, C. Guet, and H.-B. Håkansson, Towards a better parametrisation of Skyrme-like effective forces: A critical study of the SkM force, *Nucl. Phys. A* **386**, 79 (1982).
- [5] M. Kortelainen, T. Lesinski, J. Moré, W. Nazarewicz, J. Sarich, N. Schunck, M. V. Stoitsov, and S. Wild, Nuclear energy density optimization, *Phys. Rev. C* **82**, 024313 (2010).
- [6] M. Kortelainen, J. McDonnell, W. Nazarewicz, P.-G. Reinhard, J. Sarich, N. Schunck, M. V. Stoitsov, and S. M. Wild, Nuclear energy density optimization: Large deformations, *Phys. Rev. C* **85**, 024304 (2012).
- [7] M. Kortelainen, J. McDonnell, W. Nazarewicz, E. Olsen, P.-G. Reinhard, J. Sarich, N. Schunck, S. M. Wild, D. Davesne, J. Erler, and A. Pastore, Nuclear energy density optimization: Shell structure, *Phys. Rev. C* **89**, 054314 (2014).
- [8] R. Navarro Perez, N. Schunck, R.-D. Lasserri, C. Zhang, and J. Sarich, Axially deformed solution of the Skyrme–Hartree–Fock–Bogolyubov equations using the transformed harmonic oscillator basis (III) HFBTHO (v3.00): A new version of the program, *Comput. Phys. Commun.* **220**, 363 (2017).